ELSEVIER

Colloids and Surfaces A: Physicochem. Eng. Aspects 263 (2005) 33–38

COLLOIDS AND SURFACES A

www.elsevier.com/locate/colsurfa

Equilibrium conditions and symmetries for foams in contact with solid surfaces

M. Mancini*, C. Oguey

CNRS UMR 8089, Université de Cergy-Pontoise, 95031 Cergy-Pontoise, France

Received 30 September 2004; accepted 21 January 2005
Available online 20 February 2005

Abstract

The patterns formed by liquid foams in contact with solid surfaces resemble 2D foams. We derive the equilibrium equations for such 2D foams when the solid surface is curved and smooth, generalising the standard case for flat Hele–Shaw cells. The equilibrium conditions at the vertices in 2D are invariant under conformal transformations. We establish the transformation rules for films under conformal maps. Even if conformal invariance does not hold in general, by considering foams confined between two closely spaced non-parallel plates, we show that an exponential profile gives a pattern that resembles the image of a regular hexagonal foam under a complex logarithm map, to lowest order.

PACS: 82.70.Rr; 82.70.Kj; 68.03.Hj; 68.05.Gh

Keywords: Foams; Equilibrium equation; Plateau borders; Conformal map; Incidence; Contact with boundary

1. Introduction

Several recent experiments showed images of 2D foams resembling images of conformal crystals as observed in phyllotaxy [1] or in diluted suspensions of ferro-fluid balls [2,3]. In the ferro-fluid foams [4], the conformal distortion is due to gravity. [5] used special Hele–Shaw cells with an upper plate either tilted or curved. They attributed the conformal transformation behavior to volume conservation; as the thickness h varies, the 2D area of the quasi-cylindrical bubbles varies in inverse proportion. In [6], the two hemispherical walls remain parallel.

The understanding of the physical origin of this conformal behavior is not entirely clear. Below, we will prove that conformal invariance is a genuine property of the Plateau equilibrium equations at the vertices. On the other hand, the only functions conformally mapping circles to circles are the homographies, or Moebius transformations, composed of 2D similarities and inversions [7,8]. At equilibrium, since the gas pressure is constant in the bubbles, Laplace's law implies that each film has constant curvature, and hence is a circular arc in 2D. So any conformal mapping other than homographies seems to contradict Laplace's law. We propose a solution to this paradox by lifting the problem back to 3D space. Films suspended between non-parallel plates bend, with a vertical curvature contributing to the pressure balance.

Before we analyse specific cases, we formulate the equilibrium equations for the 2D foam traced out when a 3D foam contacts a solid surface. This surface may be curved, but it must be smooth and clean to prevent film pinning by irregularities and ensure relaxation to equilibrium. Otherwise, these equations hold in quite general set-ups, not only for the standard flat and parallel Hele–Shaw cell, as long as the incidence of the films or interfaces is normal[1] to the wall.

Previous studies [13,14] treated foams in curved surfaces. However, the perspective was different. The focus was mainly on coarsening due to diffusion for foams confined *in* surfaces, whence intrinsically 2D. The paradoxes raised by analysing

* Corresponding author. Tel.: +33 134256979; fax: 33 134257004.
E-mail addresses: mancini@ptm.u-cergy.fr (M. Mancini); oguey@ptm.u-cergy.fr (C. Qguey).

[1] Normal incidence is a consequence of free slip boundary conditions only if the tension along the surface is equal on both sides of the film; see Section 3. Non-normal incidence is treated in [12].

0927-7757/$ – see front matter © 2005 Elsevier B.V. All Rights Reserved.
doi:10.1016/j.colsurfa.2005.01.022

conformal images in terms of purely 2D physics led us to reconsider the problem as a contact with a boundary, involving both 2D and 3D features.

The outline of the article is as follows: After some basics on foams equilibrium in Section 2, the contacts and the equilibrium equations at the boundary are described in Section 3 for the case of normal incidence. Section 4 establishes conformal invariance for nodal equilibrium. Section 5 addresses the question of conformal mappings for the edges and solves a specific example to lowest order in non-parallelism. Section 6 concludes.

2. Foam equilibrium

Soap films obey the Young–Laplace law:

$$\Delta P + 2\gamma H = 0, \tag{1}$$

where $\Delta P = P_2 - P_1$ is the pressure difference across the film, γ is the surface tension and H is the mean curvature of the film.

Plateau showed that the films and cells meet three by three at edges and satisfy [9,10]:

$$\sum_{i=1}^{3} \gamma_i \mathbf{b}_i = 0, \tag{2}$$

$$\sum_{i=1}^{3} \gamma_i H_i = 0, \tag{3}$$

where Eq. (2) asserts that the sum of the forces on any edge is zero; the force from the film $\mathcal{F}_i$ points in the direction given by the unit vector $\mathbf{b}_i$ tangent to the film and normal to the junction. In general, the surface tension γ_j may differ on different films. A $\pi/2$ rotation around the axis tangent to the Plateau border converts the first equilibrium Eq. (2) to

$$\sum_{i=1}^{3} \gamma_i \mathbf{n}_i = 0, \tag{4}$$

where $\mathbf{n}_i$ are the normal vectors to the films.

Eq. (3) states that, by (1), the sum of the pressure drops around an edge, as on any closed path, is zero. A sign convention in (3) gives the sense of the circulation; the pressure difference in going from bubble 1 to bubble 2 is defined as $P_2 - P_1$. Via (1), this definition locally fixes the orientation of the three films around any given edge or Plateau border.

3. Contact with a boundary

Assume that the foam is in contact with a solid wall $\mathcal{S}$, smooth and clean, so that the films can freely slide along the surface.

An interface i has a contact with the wall only in non-wetting conditions; then the contact angle θ satisfies Young's law:

$$\gamma_i \cos\theta + \gamma_{S1} - \gamma_{S2} = 0, \tag{5}$$

where 1 and 2 label the two fluids (gas in normal foams) on both sides of the film.

In the case of a film – a thin double interface – the two bubbles contain the same gas so that $\gamma_{S1} = \gamma_{S2}$ and $\cos\theta = 0$. This condition of *normal incidence* is also valid when the soap solution wets the solid surface, provided the wetting films on both sides have the same surface tension.

Our purpose, next, is to see what happens if the glass surface is not planar.

3.1. Equilibrium conditions at a boundary

The contacts of the films in a 3D foam with a solid boundary $\mathcal{S}$ form a 2D foam on $\mathcal{S}$.

Consider a Plateau border ψ where three films $\mathcal{F}_i$, $i = 1, 2, 3$ meet. These films and the border contact the smooth surface $\mathcal{S}$ through a triple of lines ϕ_i and a vertex p of the 2D foam in $\mathcal{S}$ (Fig. 1). Let us parameterise the curves by arc length s with $s=0$ at p. For any curve φ, $\boldsymbol{\tau} = \dot{\boldsymbol{\varphi}} = (\mathrm{d}/\mathrm{d}s)\varphi$ is the unit vector tangent to φ.

Assume normal incidence on $\mathcal{S}$, that is, $|\theta| = \pi/2$. Then, at p, common to $\mathcal{F}_1$, $\mathcal{F}_2$, $\mathcal{F}_3$ and $\mathcal{S}$, the following hold:

$$\sum_{i=1}^{3} \gamma_i \boldsymbol{\tau}_i = 0, \tag{6}$$

$$\sum_{i=1}^{3} \gamma_i k_g(\varphi_i, \mathcal{S}) = 0, \tag{7}$$

where $k_g(\varphi_i, \mathcal{S})$ is the geodesic curvature of φ_i in $\mathcal{S}$ [11].

When all the film tensions are equal, $\gamma_i = \gamma$, the triangles representing the vector sums in (2) and (6) are equilateral and the Plateau angles are $2\pi/3$.

Because of normal incidence, the tangent $\boldsymbol{\tau}_i$ coincides with the co-normal $\mathbf{b}_i$ at p. So (6) follows immediately from (2). See ref.[12] for a full derivation of (7).

4. Conformal invariance of bidimensional foams

We may separate the equilibrium equations into two groups.

First, Laplace's equation (1) constrains the shape of the *films*. It involves the mean curvature H which we cannot, in general, determine by looking only at the contact lines with the solid surface S. One notable exception is the Hele–Shaw cell: when the foam is squeezed between *parallel* plates, flat or curved, but close to each other, the cells are cylinders, or conical sections, with zero vertical curvature. In other words, the films only curve in the direction parallel to the surface so that the geodesic curvature is proportional to the pressure

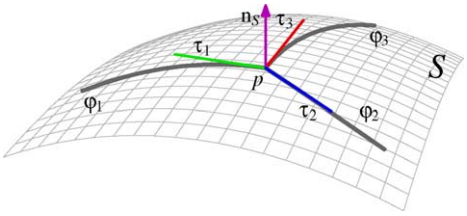

Fig. 1. The neighbouhood of a vertex p of a 2D foam: three films and a Plateau border meet at p on the solid surface $\mathcal{S}$.

difference:

$$P_2 - P_1 = 2\gamma H = \gamma k_g. \tag{8}$$

The second group comprises the two Plateau equations (6) and (7) which specify the equilibrium conditions at the *nodes* of the 2D foam. These equations somehow decouple from the full 3D problem. If we reduce the constraints to these nodal equations, then they are conformally invariant; the image of any solution, after applying a conformal map f, is still a solution, as we show in this section. As a further generalisation, the property turns out to be true for any vertex degree d (or coordination number). Plateau says that $d = 3$ in foams, but we can replace 3 by d in the equilibrium equations (6) and (7).

Explicitly, we will prove the case where both the original and image surfaces are flat, allowing us to use complex notation. Taylor expansion around the Plateau node straightforwardly extends this proof to smoothly curved surfaces.

After a brief review of curves and conformal maps in the plane (Sections 4.1 and 4.2), we define the transformation rules for the tangent vectors and curvatures (Section 4.3). The main statement is in Section 4.4.

Afterwards, Section 5 examines in more detail how edges transform and how to recover compatibility with equilibrium.

4.1. Planar curves

Parametrised C^2 curves $\varphi : [t_1, t_2] \to \mathbb{R}^2$ (or $\mathbb{C}$), $t \mapsto \varphi(t)$ describe the edges of the graphs. Arc length is $\mathrm{d}s = |\mathrm{d}\varphi| = |\dot\varphi|\,\mathrm{d}t$. The Frenet basis is

$$\tau = \frac{\dot\varphi}{|\dot\varphi|}, \qquad \nu = \left|\frac{\mathrm{d}\tau}{\mathrm{d}s}\right|^{-1} \frac{\mathrm{d}\tau}{\mathrm{d}s} = \frac{\ddot\varphi - (\tau\cdot\ddot\varphi)\,\tau}{|\ddot\varphi - (\tau\cdot\ddot\varphi)\,\tau|}. \tag{9}$$

Vector[2] ν always points toward the centre of curvature. Let us introduce another normal vector $n = I\tau$, where

$$I = \begin{pmatrix} 0 & -1 \\ 1 & 0 \end{pmatrix},$$

so that (τ, n) forms a direct basis.

[2] *Notation*: because of the identification with complex numbers, 2D vectors are not typed boldface.

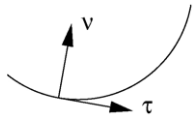

Fig. 2. The Frenet basis of a curve.

Using $\mathrm{d}|\dot\varphi|/\mathrm{d}t = \tau\cdot\ddot\varphi$, we obtain the curvature vector:

$$kn = |k|\nu = \frac{\mathrm{d}\tau}{\mathrm{d}s} = \frac{\ddot\varphi - (\tau\cdot\ddot\varphi)\,\tau}{|\dot\varphi|^2} = \frac{\nu\cdot\ddot\varphi}{|\dot\varphi|^2}\,\nu, \tag{10}$$

and the (scalar) curvature:

$$k = \frac{n\cdot\ddot\varphi}{|\dot\varphi|^2}. \tag{11}$$

Notice that $n\cdot\nu = \mathrm{sign}(k)$; $k > 0$ if the centre of curvature C is on the left of the curve, as in Fig. 2; $k < 0$ if C is on the right, assuming that τ orients the curve, in the direction of increasing t.

4.2. Conformal maps

The twice differentiable map $f : \mathbb{R}^2 \supseteq D \to \mathbb{R}^2$, defined as

$$x = \begin{pmatrix} x^1 \\ x^2 \end{pmatrix} \mapsto \tilde x = f(x) = \begin{pmatrix} f^1(x^1, x^2) \\ f^2(x^1, x^2) \end{pmatrix}, \tag{12}$$

is conformal if and only if its Jacobian matrix $J^j_{\mathrm{k}} = \partial_{\mathrm{k}} f^j$ satisfies

$$J^\dagger J = \lambda^2\, 1 \tag{13}$$

for some positive $\lambda = \lambda(x)$.

2D conformal maps are equivalent to complex holomorphic functions through the identification $\mathbb{R}^2 \leftrightarrow \mathbb{C}$,

$$x = \begin{pmatrix} x^1 \\ x^2 \end{pmatrix} \leftrightarrow z = x^1 + \mathrm{i}x^2.$$

Indeed, the Cauchy–Riemann condition,

$$\partial_{z^*} f = \tfrac{1}{2}(\partial_1 + \mathrm{i}\partial_2)(f^1 + \mathrm{i}f^2) = 0, \tag{14}$$

is equivalent to (13). Then

$$f'(z) \equiv \partial_z f = \tfrac{1}{2}(\partial_1 - i\partial_2) f = f^{1\prime} + \mathrm{i}f^{2\prime}, \tag{15}$$

where $f^{1\prime} = \partial_1 f^1 = \partial_2 f^2$, $f^{2\prime} = \partial_1 f^2 = -\partial_2 f^1$.

The scalar product in $\mathbb{R}^2$ translates as $x\cdot y = \mathrm{Re}(x^* y) = \mathrm{Re}(xy^*)$ for any complex x, y.

4.3. Paths under conformal maps

Consider a path φ and its image $\tilde\varphi$ under a conformal mapping $f : \varphi : [t_1, t_2] \ni t \mapsto \varphi(t) \overset{f}{\mapsto} \tilde\varphi(t) = f(\varphi(t)) \in \mathbb{C}$. The transformation rules are:

$$\dot{\tilde\varphi} = f'\,\dot\varphi, \tag{16}$$

$$\ddot{\tilde{\varphi}} = f'\,\ddot{\varphi} + f''(\dot{\varphi})^2, \tag{17}$$

$$\tilde{\tau} = \frac{f'}{|f'|}\,\tau, \qquad \tilde{\nu} = \frac{f'}{|f'|}\,\nu, \qquad \tilde{n} = \frac{f'}{|f'|}\,n, \tag{18}$$

$$\tilde{k} = \frac{\mathrm{i}\tilde{\tau}\cdot\ddot{\tilde{\varphi}}}{|\dot{\tilde{\varphi}}|^2} = \mathrm{i}\frac{f'}{|f'|}\tau\cdot\frac{f'\ddot{\varphi}+f''(\dot{\varphi})^2}{|f'\dot{\varphi}|^2}$$
$$= \frac{1}{|f'|}\left(k + \mathrm{Re}\left[-\mathrm{i}\frac{f''}{f'}\tau\right]\right), \tag{19}$$

where $f' \equiv f'(\varphi(t))$, etc.

4.4. Conformal invariance of nodal equilibrium

Let $X = (V, E, \gamma)$ be a graph in the plane with vertex set V, edges E (all twice differentiable curves) and line tensions $\gamma : E \to \mathbb{R}$.

For any conformal map f of the plane, the Plateau conditions ((6) and (7)) are satisfied at all vertices of $\tilde{X} = f(X)$ if and only if they are satisfied by X.

To check this proposition, let x be a vertex of the graph and $\tilde{x}$ its image; x is a point common to all the edges ϕ_j incident on it, $j = 1, \ldots, \mathrm{d}$.

The equivalence for (6) is an immediate consequence of conformality: let $\mathrm{e}^{\mathrm{i}\theta(x)} = f'(x)/|f'(x)|$; then, by (18), $\sum \gamma_j\,\tilde{\tau}_j = \mathrm{e}^{\mathrm{i}\theta}\sum \gamma_j\,\tau_j$, showing that condition (6) for $\tilde{x}$, $\{\tilde{\tau}_j\}$ holds if and only if it holds for x, $\{\tau_j\}$.

To show that (7) for $\tilde{x}$ is equivalent to (7) for x, we may use (19):

$$\sum_{j=1}^{\mathrm{d}} \gamma_j\,\tilde{k}_j = \frac{1}{|f'|}\left(\sum \gamma_j\,k_j + \mathrm{Re}\left[-\mathrm{i}\frac{f''}{f'}\sum \gamma_j\,\tau_j\right]\right), \tag{20}$$

where everything is evaluated at x. Using (6), we see that the sum of the curvatures around $\tilde{x}$ vanishes if and only if the sum around x does.

Drenckhan et al. [5] gave an alternative argument, based on homographies and Taylor expansion to second order.

5. Mapping the edges: the example of the log

In the previous sections, we have seen that the equilibrium conditions at the nodes are invariant under conformal maps. Here, we consider the effect of a specific conformal map on the edges. The logarithmic map is one of the examples experimentally demonstrated in [5]:

$$F(z) = \frac{1}{\mathrm{i}\alpha}\ln(\mathrm{i}\alpha z), \tag{21}$$

where α is a real parameter. This mapping is also relevant to gravity arches observed in ferro-fluid suspensions under gravity [2,3] and to ferro-fluid 2D foams [4]. The logarithm is the only conformal map translationally invariant [2,3,15].

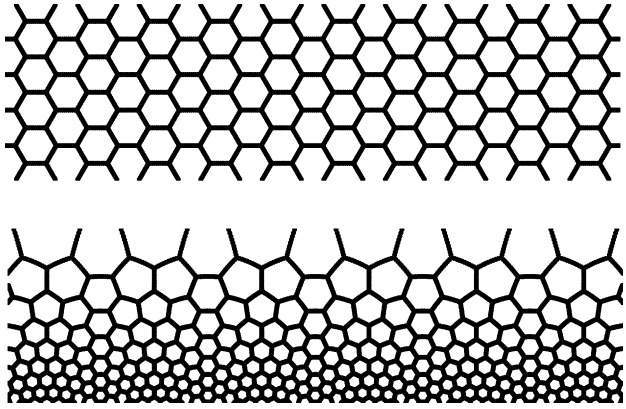

Fig. 3. The regular hexagonal foam and its image under the log map.

Under mappings such as the logarithm, the image of a circular arc is not a circular arc. We first evaluate the curvature to see how close the curve is to a circle. Then we will argue that, in the circumstances under study, the edges do not need to be circular to satisfy the equilibrium conditions. Under gravity, as in [4], we must add the gravity field to the edge equations (1) or (8). When the foam lies between two non-parallel plates, curvature in the third dimension modifies the equations with respect to the usual 2D formulae, as explained below (Section 5.2).

5.1. Log map of an edge

The inverse $f(z) = F^{-1}(z) = \exp(\mathrm{i}\alpha z)/\mathrm{i}\alpha$ maps a foam X in a non-parallel chamber to a reference one, $\tilde{X}$. The function f satisfies $f' = \mathrm{i}\alpha f$. Inverting Eq. (19) and applying it to f gives the curvature vector:

$$k = \tilde{k}|f'| + \mathrm{Re}\left[\mathrm{i}\frac{f''}{f'}\tau\right] = \alpha\left(|\tilde{\varphi}|\tilde{k} - \mathrm{Re}[\tau]\right). \tag{22}$$

In (22), the first term on the right is the effect of the local scale change by $|f'|$; according to the second term, edges nearly parallel to the imaginary axis are almost undeformed, up to similarities, whereas those parallel to the real axis bend. See Fig. 3.

5.2. Foam between non-parallel plates

Suppose that the foam is sandwiched between two plates, as in a conventional Hele–Shaw cell, except that the upper plate is not parallel to the bottom one, as in [5]. We may describe the upper plate face wet by the foam by a height function $h(x^1, x^2)$ defined in the plane at the bottom of the cell. We assume that both h and its slope $|\nabla h|$ are small. The 2D vector ∇h locally indicates the direction of maximal slope. The slope in this direction is the local dihedral angle (which is small). Because the film meets both top and bottom faces orthogonally, it must curve: its sectional, or normal, curvature in the vertical direction is $k_{\mathrm{v}} \simeq -\mathbf{n}_{\mathcal{F}}\cdot\nabla h/h$ (Fig. 4). At the same degree of approximation, we can approximate the

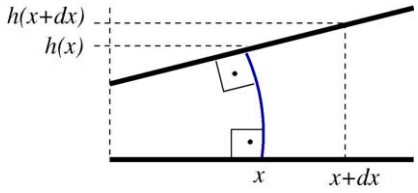

Fig. 4. A film joining two non-parallel plates.

mean curvature H by adding the horizontal sectional curvature, which is nearly the geodesic curvature $k \equiv k_g(\varphi, \mathcal{S})$ of the curve $\varphi = \mathcal{F} \cap \mathcal{S}$, $\mathcal{S}$ being the upper or lower boundary. Then, Laplace's law says

$$P_1 - P_2 = 2\gamma H_{\mathcal{F}} = \gamma(k + k_v) \simeq \gamma\left(k - \frac{\mathbf{n}_{\mathcal{F}} \cdot \nabla h}{h}\right). \quad (23)$$

Thus, in equilibrium, with pressure difference constant along the film, the geodesic curvature differs from a constant by the last term in (23), representing contributions from curvature in the third direction.

Example

Consider the exponential profile $h(z) = h_0 \exp(g \cdot z)$, where g is a fixed small vector in the bottom plane. In this case $k_v \simeq -g \cdot n$.

The exponential profile gives a contribution matching that of the log map if we take $g = -i\alpha \leftrightarrow (0, -\alpha)$. Indeed, as $\mathbf{n}_{\mathcal{F}} \simeq n = i\tau$, $k_v \simeq -g \cdot n = \mathrm{Re}[\alpha\tau]$. Comparing (22) and (23), we get: $\alpha|\tilde{\varphi}|\tilde{k} = (P_1 - P_2)/\gamma$. If the reference flat foam is at constant pressure ($\tilde{k} = 0$), e.g. a hexagonal foam [5], we conclude that the conformal image between non-parallel plates is also at constant pressure; a vertical contribution, invisible in the projection, compensates the curvature apparent in the 2D projection.

6. Conclusion

When a foam is in perpendicular contact with a smooth solid surface, the 2D foam formed by the contacts satisfies the 2D Plateau equilibrium conditions at the nodes. The case of oblique, non-normal incidence is more involved and no simple separation appears to occur of the 2D from the 3D problem.

The equilibrium equations for the nodes, (6) and (7), are conformally invariant, as we have proved in Section 4.

While films are circular arcs in standard 2D foams, they may deform, either under external fields such as gravity or electromagnetic forces, or when the container wall is not flat. In fact, the pressure difference is the sum of two curvatures. Along a contact curve, these may be the geodesic (longitudinal) and normal curvatures, which can both vary along the curve even if the sum, $2H$, is constant. For a chamber bounded by two smooth, non-parallel plates, with exponential profile, the 2D conformal image has non-constant geodesic curvatures k_j but Laplace's law nevertheless holds, provided we consider the films as curved surfaces in space.

However, comparison with the available experiments is not straightforward. The transformations of [5] were done at constant bubble volume, implying $h \propto |f'|^2$ if the bubbles are small enough, whereas our theory, based on film equilibria, yields $h \propto |f'|$, but at constant pressure. Except for the trivial case where the plates are parallel, these relations differ.

Is our assumption of nearly constant vertical curvature too crude? Another possibility is that the precise mappings describing the geometry at long and short length scales might differ. One mapping, e.g. obeying the constant volume or constant pressure condition, would describe the global order, the bubbles arrangement, in a way similar to that for magnetic suspensions [2]; whereas the local geometry, at the scale of individual films or bubbles, would agree with another mapping following from the local equilibrium conditions as we have shown. This point is further discussed in [12].

Combining these two length scales raises challenging questions. Similar experiments carried out at constant pressure rather than constant volume would be interesting.

The integral of the geodesic curvature is one of the contributions to the Gauss Bonnet theorem. For intrinsically 2D foams, this term sums up to a topological quantity in the evolution equation [16]. Another contribution is the integrated Gaussian curvature [13,14]. There were also proposals to find 3D analogues of von Neumann's law [13,17]. How the foam coarsens near a solid, impermeable, wall is yet an interesting question.

Acknowledgements

We would like to thank D. Weaire for discussions and showing us pictures of [5] prior publication, and N. Rivier for an avalanche of helpful suggestions.

References

[1] R.V. Jean, Mathematical Approach to Patterns and Forms in Plant Growth, Wiley, 1984.
[2] F. Rothen, P. Pieranski, N. Rivier, A. Joyet, Eur. J. Phys. 14 (1993) 227–233.
[3] F. Rothen, P. Pieranski, Phys Rev. E 53 (1996) 2828–2842.
[4] F. Elias, J.C. Bacri, H. de Mougins, T. Spengler, Phil. Mag. Lett. 79 (1999) 389–397.
[5] W. Drenckhan, D. Weaire, S.J. Cox, Eur. J. Phys. 25 (3) (2004) 429–438.
[6] J. M. Di Meglio, T. Senden, Non Euclidean Foams, in preparation.
[7] D. Weaire, Phil. Mag. Lett. 79 (1999) 491–495.
[8] M. Mancini, C. Oguey, Phil. Mag. Lett. 83 (2003) 643–649.
[9] D. Weaire, N. Rivier, Contemp. Phys. 25 (1984) 59–99.
[10] D. Weaire, S. Hutzler, The Physics of Foams, Clarendon Press, Oxford, 1999.
[11] F. Morgan, Riemannian Geometry: A Beginner's Guide, A.K. Peters, Wellesley, MA, 1998.

[12] M. Mancini, C. Oguey, Eur. J. Phys. E (2004); http://arxiv.org/abs/cond-mat/0501334, submitted for publication.
[13] J.E. Avron, D. Levine, Phys. Rev. Lett. 69 (1992) 208–211; P. Peczak, G.S. Grest, D. Levine, Phys. Rev. E 48 (1993) 4470–4482.
[14] O. Schoenborn, R.C. Desai, J. Statist. Phys. 95 (1999) 949–979.
[15] N. Rivier, D. Reinelt, F. Elias, C. Vanden Driessche, in: D. Weaire, J.Banhart (Eds.), Proceedings of the International Workshop on Foams and Films, Leuven, Belgium, March 5–6, Verlag MIT Publishers, 1999.
[16] J. von Neumann, Metal Interfaces, American Society for Metals, Cleveland, OH, 1952 108.
[17] C. Monnereau, N. Pittet, D. Weaire, Europhys. Lett. 52 (2000) 361–367.